CONTROL OF SILICA POLYMERISATION DURING FERROMANGANESE SLAG SULPHURIC ACID DIGESTION AND WATER LEACHING

DM Kazadi[1a], DR Groot[a], JD Steenkamp[a] and H Pöllmann[b]

[a] Department of Materials Science and Metallurgical Engineering, University of Pretoria, Lynwood Road, Pretoria, 0002, Republic of South Africa

[b] Institute of Geosciences, Mineralogy/Geochemistry, Martin Luther University, Von-Seckendorff-Platz 3, Halle (Saale) 06120, Germany

Highlights

• This article will show that the quick leach model, also called the water-starved system, limits silica solubilisation and its subsequent polymerisation during manganese extraction from ferromanganese slags.

• It will further illustrate that the silica content in the residue is dependent on the acid concentration used during acid digestion. It will also show that dissolved silica in the pregnant leach solution is dependent on the quantity of water used.

• Furthermore, a method for silica gel recovery from ferromanganese slag will be presented, as well as the silica gel analysis, in order to confirm the theory presented in this article.

• The silica and calcium sulphate-rich residue can be used as an addition to Portland cement or as a gypsum replacement.

ABSTRACT

A major obstacle to the hydrometallurgical treatment of ferromanganese slags is the way in which silica polymerisation is controlled during sulphuric acid digestion and water leaching. In an acidic medium, silica enters in solution and forms silicic acid, which polymerises into silica gel and makes solid-liquid separation difficult.

This article will show that the quick leach model, also called the water-starved system, limits silica solubilisation and its subsequent polymerisation during manganese extraction from

[1] Corresponding author: E-mail address: dieudonne.kazadi@gmail.com

ferromanganese slags by rejecting most of the ferromanganese slag silica content in the leach residue. It will further illustrate that the silica content in the residue is dependent on the acid concentration used during acid digestion. It will also show that dissolved silica in the pregnant leach solution is high when an unrestricted quantity of water is used and low when the water quantity is restricted during water leaching. Furthermore, a method for silica gel recovery from ferromanganese slag will be presented, as well as the silica gel analysis, in order to confirm the theory presented in this article.

Manganese extraction of up to 90% is obtained and the leach residue presents good latent hydraulic properties, which can be used as an addition to Portland cement or a gypsum replacement. More than 95% of the initial silica content of the slag is rejected in the leach residue, and a residue silica content of more than 27% is obtained. Thus, silica solubilisation and polymerisation is controlled and solid-liquid separation accelerated.

Key words: Silica, silica gel, polymerisation, ferromanganese, slags, leaching, manganese, leach solution, leach residue, Portland cement

1. Introduction

Ferromanganese slags contain silicate phases. The covalent bond between silicon and oxygen in silicates is a strong bond that cannot be easily broken by aqueous solutions (Habashi, 1993). The destruction of silicate structures by acid occurs as a result of the dissolution of metals present in the structure. This dissolution results in the collapse of the three-dimensional silicate structure to form silicic acid (Parris, 2009).

Silicate minerals attacked with acid either gelatinise or separate into insoluble silica. Those which gelatinise are (Murata, 1943):

- Those containing silicate radicals of small molecular weight, and possibly silicates containing ring structures of three silicon atoms (such as orthosilicates, pyrosilicates);

- Those containing large continuous silicon-oxygen networks (disilicates containing appreciable ferric iron in the silicon-oxygen sheets, and minerals of the silica type with three-

dimensional networks that contain aluminium in a ratio of at least two aluminium atoms to three silicon atoms); and

- Those which separate into insoluble silica are characterised by silicon-oxygen structures of large dimensions that do not disintegrate into small units under acid attack, such as SiO_8 chains, SiO_{11} chains, and Si_2O_5 sheets that do not contain large amounts of ferric iron that replace silicon, and three-dimensional networks that have an aluminium content lower than the ratio of two aluminium atoms to three silicon (Murata, 1943).

In order to solubilise valuable silicates for metal recovery, a thermal treatment is usually required before leaching (Habashi, 1993).

Silica polymerisation is a major problem during ferromanganese slag acid leaching as it makes filtration difficult afterward. This article presents techniques on how to deal with silica polymerisation, and uses the quick leach or water-starved model described by Dufresne (1976). This model is used to minimise silica polymerisation, and concentrated sulphuric acid is used because of its ability to destroy the structure of the silicate phase by dissolving metals in the structure.

In the available literature, little is reported in terms of work focused on the leaching of ferromanganese slags in sulphuric acid in order to recover manganese values and to limit silica polymerisation. Past investigations are described elsewhere (Kazadi *et al*., 2013). Of great interest to this study is the work of Das *et al*. (1986). Das *et al*. did some leaching work on ferromanganese slags using hydrochloric acid and sulphuric acid at different temperatures, ranging from room temperature to 99^{o}C. Silica gel polymerisation was observed as being a major problem during filtration. The effects of acid quantity, temperature, leaching duration, solid-liquid ratio and particle size, were studied. An extraction of 90% manganese was achieved, but silica polymerisation is not addressed.

2. Silica polymerisation

Silica has different degrees of crystallisation, exhibiting different solubilities in aqueous solutions. The highest degree of solubility is exhibited by amorphous silica (Queneau and Berthold, 1986) – the form of silica which is precipitated from aqueous solution and which is also present in the leach residue of ferromanganese slags (Kazadi *et al*., 2013).

Thermodynamically, in acidic solution, soluble silica is present as the monomer silicic acid $Si(OH)_4$, as seen in the Eh-pH diagram of silica in water (Figure 1). Figure 2 provides the solubility of amorphous silica in aqueous solution as a function of pH. In practice, 100 to 200 mg/l as SiO_2 is assumed to be the solubility range of amorphous silica in acidic medium (depending on particle size, state of internal hydration, and the presence of impurities absorbed in the silica or on its surface) (Iler, 1979). However, in acidic solution, silica concentrations in excess of the equilibrium solubility of monomeric silica are encountered, which is also known as supersaturated solution. The ageing of these solutions results in the formation of amorphous silica, either in the form of a colloid or a gel, called silica gel (Queneau and Berthold, 1986). It must also be noted that a supersaturated silica solution can remain crystal clear for a long period of time due to the silica gel's optical properties in solution (Parris, 2009).

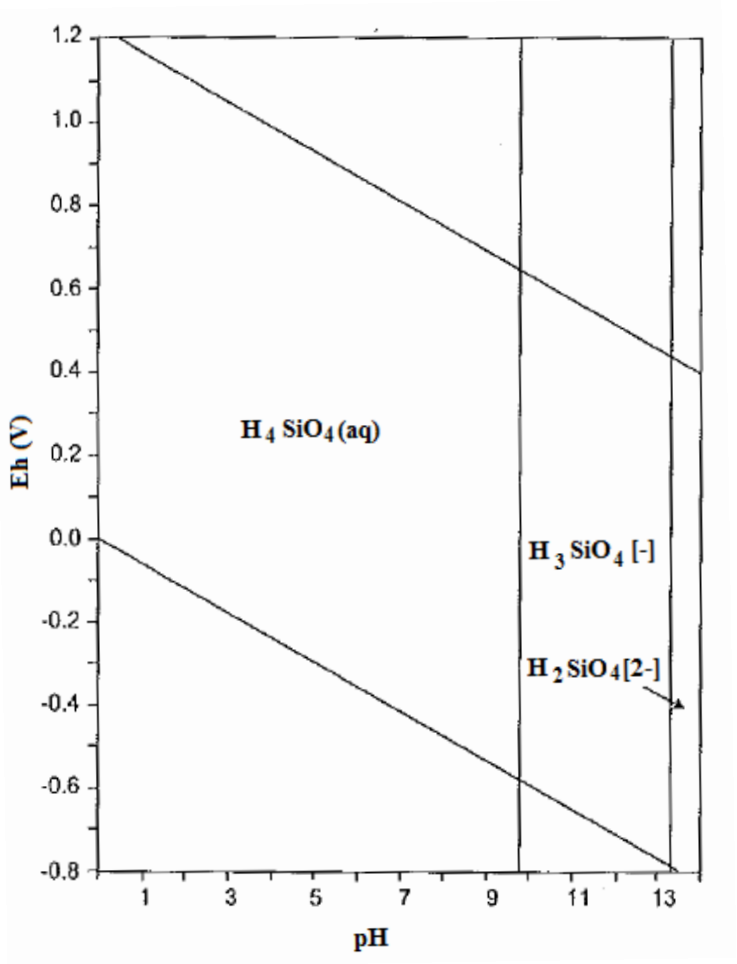

Figure 1. Eh-pH diagram of the system Si-O-H at 298.15 K and 100 kPa (Takeno, 2005)

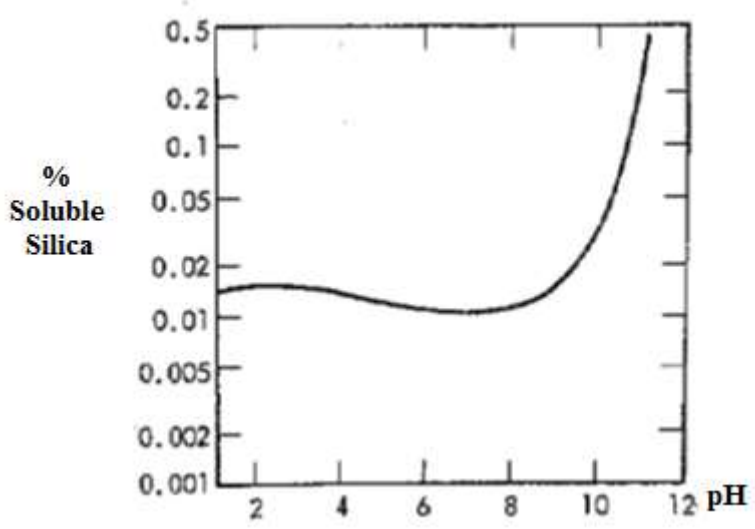

Figure 2. Amorphous silica solubility in water at 25°C (Queneau and Berthold, 1986)

Silica gelling is caused by the rapid polymerisation of silicic acid to form open networks. It causes dramatic increases in both plastic viscosity and yield stress that cannot be reversed by dilution. In brief, silica gel forms when silicic acid aggregates in a manner that incorporates most, if not all, of the water.

The chemistry of silica gel formation can be simply represented by:

$$nSi(OH)_4 = (SiO_2)_n + 2nH_2O \quad (1)$$

The iso-electric point of colloidal silica is pH 2. Above this point, colloidal silica is negatively charged, and below it, it is positively charged. Silica is amphoteric and always carries both charges on its surface. Below pH 2, colloidal silica grows by coalescence, which is a chaotic process and can be very fast. This growth results in a wide range of particle sizes, as well as precipitated silica and, in special cases, silica gel (Parris, 2009).

3. Quick leach chemistry (Dufresne, 1976)

The chemistry of the quick leach is based on a water-starved system and effectively rejects silica from various silicate materials.

In the case of a divalent metal silicate, such as M_2SiO_4, when attacked by sulphuric acid in the presence of excess of water, the reaction will be:

$$M_2SiO_4 + 2H_2SO_4 + \infty\ H_2O \rightarrow 2M^{2+} + 2SO_4^{2-} + \infty\ H_2O + Si(OH)_4\ (gel) \quad (2)$$

If water is restricted, the reaction will then be:

$$M_2SiO_4 + 2H_2SO_4 + nH_2O \rightarrow 2MSO_4.\ nH_2O + Si(OH)_4 \quad (3)$$

The partially hydrated metal sulphate then further reacts with silicic acid as follows:

$$2MSO_4.\ nH_2O + Si(OH)_4 \rightarrow 2MSO_4.\ (n+2)H_2O + SiO_2\ (filterable) \quad (4)$$

Thus, the overall reaction is:

$$M_2SiO_4 + 2H_2SO_4 + nH_2O \rightarrow 2MSO_4.\ (n+2)H_2O + SiO_2\ (filterable) \quad (5)$$

It is said that in a water-deficient system, the sulphate produced in the reaction indicated by equation (5) scavenges the available water, thus leaving little or none for the hydration of the silica for its polymerisation, and thus limiting silica polymerisation. The dehydrated silica species produced by reaction (5) is readily filterable.

4. Material and methods

4.1. Material

Manganese ferroalloys are produced by a carbothermic reduction process. This involves the reduction of manganese ores by solid carbon reductants to produce an alloy, slag and off-gas. From a slag chemistry perspective, the slag utilised in this investigation is a discard slag from high carbon ferromanganese production (HCFeMn) (Steenkamp and Basson, 2013), and originated from a South African ferromanganese producer. Furthermore, all the chemical reagents used for this investigation were of analytical grade.

4.2. Instrumentation

The following instruments were used for analysis:

-Thermo ARL9400XP spectrometer: X-ray fluorescence (XRF) analysis

- PANalytical X'Pert Pro diffractometer; X-ray diffractometry (XRD) with X´celerator detector and Highscore Plus software

-Spectro Arcos model inductively coupled plasma optical emission spectrometer (ICP-OES)

-Thermo Scientific ICE 3000 AA spectrometer

-Bruker QUANTAX EDS for scanning electron microscopy (SEM).

4.3. Material Characterisation

The ferromanganese slags were collected from a South African ferromanganese producer's slag heap. These were obtained in a coarse form, equivalent to 3 to 5 cm in diameter. The slag was first crushed in both jaw and cone crushers, before being milled in a ball mill to less than 300 µm, and thereafter mixed and homogenised in a rotary splitter. Additionally, particle size analysis was performed using a vibrating sieve shaker.

4.4. Leaching method

Except when stated otherwise, the leaching method below was applied in the majority of the experiments and is the standard leaching method of this work. A 100 g of milled ferromanganese slag was pre-mixed with 100 ml of water. The milled ferromanganese slag slurry was digested in 100 ml of concentrated sulphuric acid. The quantities of the slag and sulphuric acid were determined by calculating their stoichiometric quantities, and also according to Lindblad and Dufresne (1975). The reaction between the ferromanganese slag and sulphuric acid was instantaneous and very exothermic. The slurry solidified as a cake after a few minutes. This cake was left to age overnight in order to slightly increase manganese recovery (Dufresne, 1976).

After ageing, the cake was broken and subjected to agitation leaching in 400 ml of water. The amount of water had to be kept at a minimum in order to avoid hydration, and the concomitant polymerisation of the silica (Dufresne, 1976). The quantity of water was chosen after trials as will be shown in section 5.5. It is important that the concentration of manganese will be compatible with manganese solubility in water, and subsequently compatible with conventional downstream processes.

The pregnant leach solution and the insoluble leach residue were separated by filtration through the use of a pressure filter. The insoluble leach residue was washed four times on the pressure filter cloth with equal additional 400 ml of fresh water each time to remove any residual manganese, and then dried in an oven at 105^{o}C.

5. Results and discussion

5.1. Ferromanganese slag chemical and phase analysis

Table 1 provides the typical chemical compositions of the ferromanganese slag used in this investigation. These were obtained through the use of X-ray fluorescence (XRF) analysis of the major and minor elements of three subsamples. The analysis was repeated at different times during the course of the test work campaign in order to test for the reproducibility of results. As can be seen in Table 1, the results show some variations, which is not surprising for a residue material. From the analysis, it is also clear that silicon, manganese, calcium and aluminium are the major constituents. Iron, which is usually an undesirable impurity in downstream metallurgical processes, is low.

Table 1. Typical chemical analysis of ferromanganese slag used in this study

Oxide	Mass composition [%]		
	Sample 1	Sample 2	Sample 3
SiO_2	30.1	31.2	29.2
Al_2O_3	4.8	4.4	3.9
Fe_2O_3	1.4	0.8	0.8
MnO	27.9	26.7	25.6
MgO	6.5	6.5	6.9
CaO	28.4	30.5	28.3
SO_3	2	0	3.6

In Table 2, the typical mineral composition of the ferromanganese slag obtained by X-ray diffraction (XRD) is tabulated for two subsamples taken at different times during the test work campaign. Figure 3 presents a typical XRD spectrum of the ferromanganese slag used in this study. XRD analysis was also repeated to verify the reproducibility of results. The results of the XRD analyses, like the XRF results, also show some variations, which is expected for a residue material. The XRD analysis was done with the use of the Rietveld refinement technique, and 20% silicon was added as an internal standard in order to determine the amorphous content of the slag. The major phases in the ferromanganese slags are silicates. As can be seen in Table 2, the amorphous content of the ferromanganese slag is high, approximately 30%. Silica in the ferromanganese slag is present as a double silicate of calcium and manganese in glaucochroite, a double silicate of magnesium and calcium in monticellite, and a tetragonal sorosilicate in gehlenite.

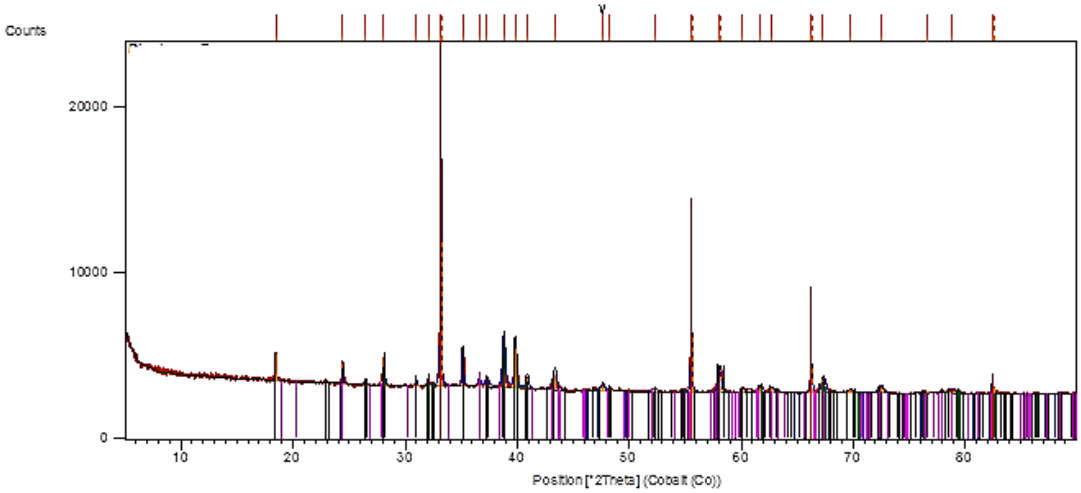

Figure 3. XRD spectrum of ferromanganese slag (Silicon (20%) was added as internal standard for the determination of amorphous content)

Based on the XRD analysis example in Table 2 (specifically sample 2, although the same can be done with sample 1), a mass balance was performed and the results are provided in Table 3. The first column of this table shows the XRF analysis results of the sample. The amorphous content, as determined in Table 3, was calculated using the XRD and XRF analysis. From the XRD and XRF mass balance, one can clearly see that manganese in the amorphous phase of the ferromanganese slag is 4.9% (as MnO) and silica in the amorphous phase is 4.7% (as SiO_2), but the highest amorphous content is exhibited by calcium at 7.2% (as CaO). The calculations, and the assumptions made therein, were done according to Loubser and Verryn (2008). This mass balance was done with the idea of an in-depth characterisation of the ferromanganese slag, in order to distinguish the amorphous or glassy phase from the crystalline phase; the more reactive part of the ferromanganese slag to the less reactive part.

Table 2. Typical phase analysis of the ferromanganese slag

Mineral	**Quartz**	**Monticellite**	**Gehlenite**	**Glaucochroite**	**Graphite**	**Manganosite**	**Amorphous content**
Chemical structure	SiO_2	$CaMgSiO_4$	$Ca_2Al[AlSiO_7]$	$CaMnSiO_4$	C	MnO	
	[%]	[%]	[%]	[%]	[%]	[%]	[%]
Sample 1			7.2	58.6	2.2	2.5	29.5
Sample 2	1.3	1.8	4.4	63.6			29.1

Table 3. Mass balance analysis of ferromanganese slag based on XRD and XRF analyses

Element	Total Content [XRF, %]	Crystalline Content [XRD, %]	Amorphous Content [%]
SiO_2	27.9	23.2	4.7
CaO	28.4	21.2	7.2
MnO	29.0	24.1	4.9
MgO	6.3	0.5	5.8
Al_2O_3	5.5	1.6	3.9
TiO_2	0.2		0.2
Fe_2O_3	1.1		1.1
Na_2O	0.3		0.3
K_2O	0.2		0.2
SO_3	0.35		0.35
BaO	0.7		0.7
Total	100.0	70.6	29.4

5.2. Ferromanganese slag particle size analysis and silica content

Figure 4 shows the cumulative mass percentage of the milled ferromanganese slag's particle size distribution. Chemical analysis (as determined by XRF) of the size fractions shows that the silica content is evenly distributed, but slightly high in the size range of 200 to 400 µ. As it will be shown in a future publication, this is the particle size range in which optimal leaching of manganese from ferromanganese slag is obtained experimentally.

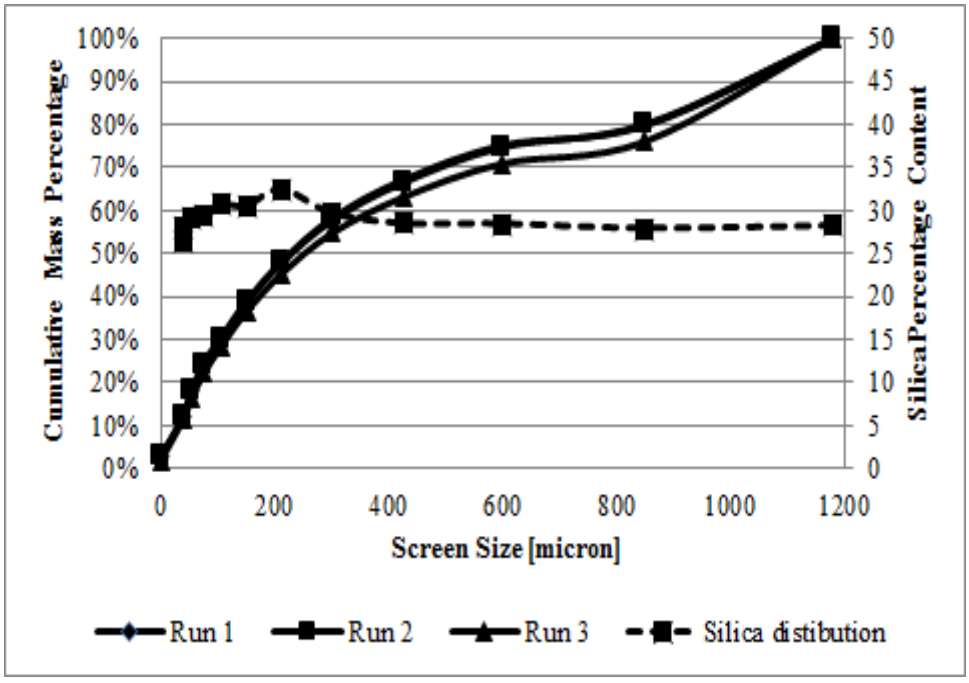

Figure 4. Silica distribution in ferromanganese slag and size distribution

5.3. Pregnant leach solution analysis

The manganese content in the pregnant leach solution is high at 60 g/l. This relates to a recovery in excess of 90%, based on solid and solution analysis. Table 4 presents a typical analysis of the pregnant leach solution for elements other than manganese. The manganese concentration is higher than 30 g/l, which is the minimum recommended concentration, and iron and silicon contents must be reduced to lower than 15 and 10 mg/l respectively, if it is to be used for manganese electrowinning (Harris *et al*., 1997; Sancho *et al*., 2009). Manganese electrowinning is done at approximately pH 7 and, at that pH, silica and iron in solution will be precipitated (Harris *et al*., 1997; Sancho *et al*., 2009).

Table 4. Typical concentrations of different elements in the pregnant leach solution, determined by ICP

Na	Mg	Al	K	Ca	Fe	Si
[mg/l]	[mg/l]	[mg/l]	[mg/l]	[mg/l]	[mg/l]	[g/l]
15 - 20	4 - 6	1 -2	1 -5	75 -80	240-250	0.8 – 1.4

5.4. The effect of sulphuric acid concentration on residue silica content

It was observed experimentally that the silica content of the leach residue, is dependent on the concentration of sulphuric acid solution used during digestion (Figure 5), thus confirming the chemistry of the quick leach model (Dufresne, 1976), that the majority of the silica in ferromanganese slag is rejected in the residue as filterable microsilica. In these experiments, the stoichiometric mass of sulphuric acid was calculated, then it was diluted in water in order to obtain the desired sulphuric acid concentration, then mixed with 100 g of dry ferromanganese slag, before being leached in 400 ml of water.

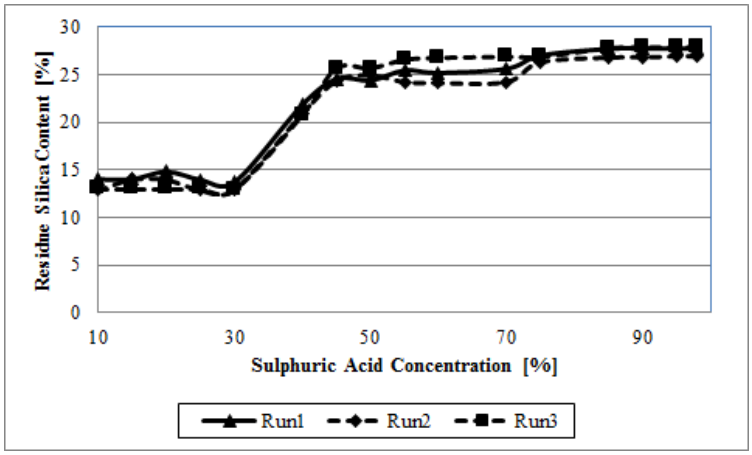

Figure 5. Residue silica content as a function of acid concentration (based on XRF analysis) used during ferromanganese slag digestion

5.5. The effect of water quantity used during leaching on dissolved silica

The extent to which silica dissolved in the pregnant leach solution was proportional to the quantity of water used during cake water leaching. In the case of a small quantity of water being used, it was found that the level of dissolved silica was also low. If an unlimited quantity of water was used, it was found that the level of dissolved silica was high, and the probability of silica polymerisation was also high. This is shown in Figure 6. In these experiments, the standard leaching method as described in section 4.4 was used. However the resultant cake was water-leached in different quantities of water, varying from 100 ml to 1600 ml. The trend observed here is in agreement with those observed by Dufresne (1976) and Baumgartner and Groot (2013). This observation confirms the quick leach or water-starved model. It can also be used for the production of silica gel from ferromanganese slags and, at the time of writing this article, a patent was being filled by the authors. It must be noted that solution analysis was performed on fresh solutions (Parris, 2009). Based on the analysis of the experiments, it is clear that the use of 1000 ml or more water during water leaching will likely lead to the formation of silica gel in solution.

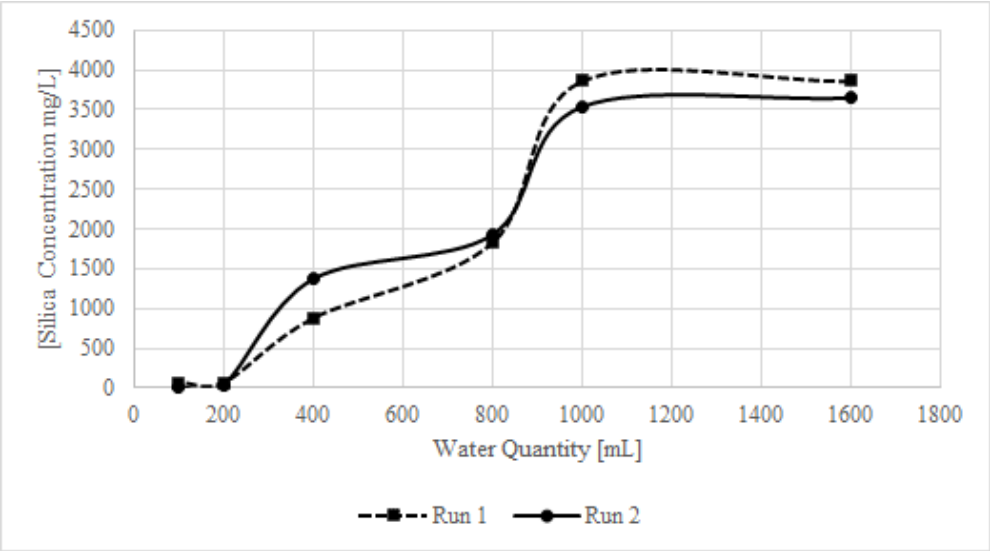

Figure 6. Dissolved silica content as a function of water quantity used during water leaching, based on ICP – OES analysis

5.6. The effect of the number of washing stages on dissolved silica

Table 5. Silica distribution mass balance after the leaching of ferromanganese slag

Feed FeMn Slag [g]	Solution [g]	Residue [g]	% Silica in residue	% Silica in solution
27.5	0.7	26.8	97.3%	2.7%
27.5	0.2	27.3	99.2%	0.8%

Table 5 provides the mass balance of silica for a sample digested and leached under the standard experimental conditions of this study. It is clear that more than 95% of the silica was rejected in the residue and only 0.8 to 3% of silica was dissolved in the pregnant leach solution. The concentration of silica in solution (0.8 to 1.4 g/l) was higher than the silica solubility range (100 to 200 mg/l) at pH less than 1. These are, therefore, silica supersaturated solutions.

However, it has been observed that 70 to 80% of the silica that goes in solution does so during water leaching. Only 20 to 30% of the solubilised silica goes in solution during washing. After the fourth wash, the silica in solution is approximately zero. Figure 7 illustrates this graphically (Stage 0 on the graph represents the leaching stage).

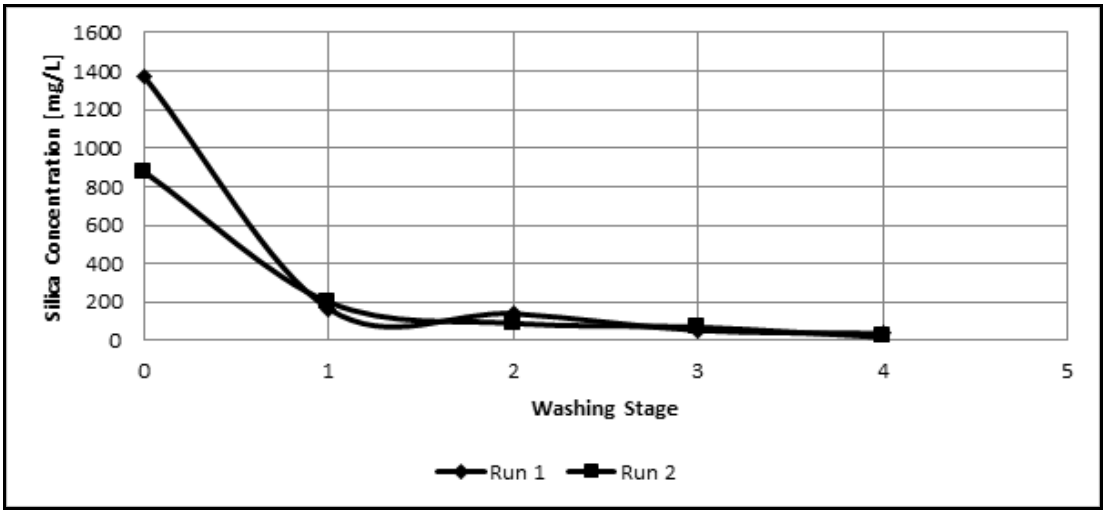

Figure 7. Dissolved silica as a function of the washing stage (based on ICP-OES analysis).

5.7. Gel Analysis

If low sulphuric acid solution concentrations are used during ferromanganese slag digestion, a gel is produced during cake maturation. During water leaching, if an excessive quantity of water is also used, a gel is obtained in solution after a few hours. It was also observed that leaching freshly tapped slag produces a gel more easily than slag obtained from a slag heap. The different gels obtained during the test work campaign were mixed in a beaker. The sample selected for analysis was dried at 100^{o}C and then milled. Tables 6 and 7 respectively provide the chemical and phase analyses of two impure dried gel samples. These subsamples were also taken randomly during the test work campaign in order to verify the reproducibility of results. The gel's major constituents are silica, manganese and, to an extent, magnesium

and aluminium. The silica in the gel is amorphous. It is clear that the gel is an impure silica gel contaminated by manganese sulphate, magnesium sulphate and other impurities. Manganese sulphate is the more abundant impurity due to the fact that the gel was formed in a manganese sulphate medium. The high loss on ignition (LOI) is due to the water's association with the silica during polymerisation. The gel obtained can be washed, calcined, or roasted and used in ceramics, as well as in cement and concretes (as an accelerator to develop their strength). It can also be used for the synthesis of zeolites, as proposed by Seggiani and Vitolo (2003), for silica gel obtained from blast furnace slag. After washing and purification, the gel can also be used as a desiccant, absorbent, coatings, catalysts or catalyst carriers (Habashi, 1997). In Figure 8, the XRD spectrum of the dried silica gel is presented.

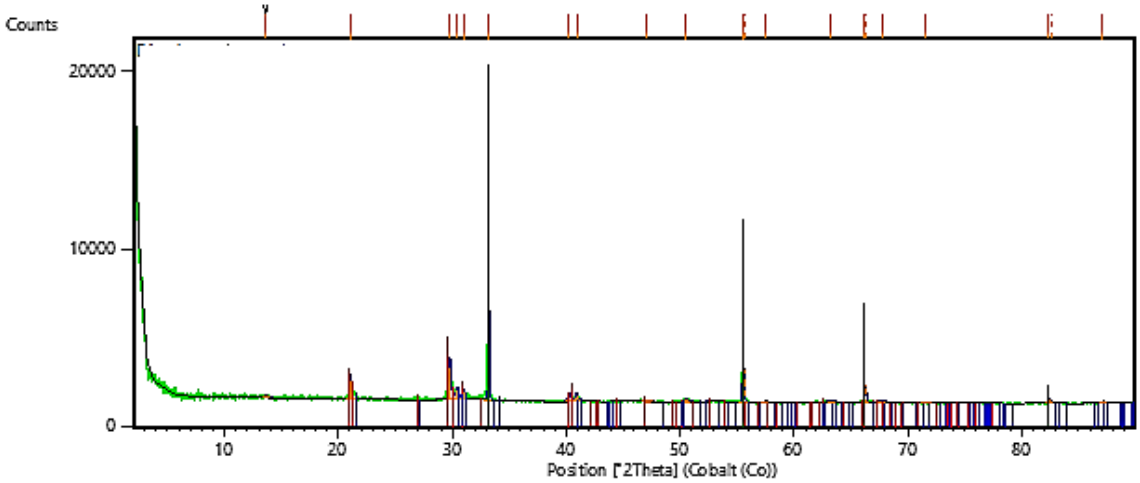

Figure 8. XRD spectrum of dried silica gel (Silicon (20%) was added as internal standard for the determination of amorphous content)

Table 6. Dried gel chemical composition by XRF analysis

Oxide	Weight Percentage	
	Sample 1	**Sample 2**
LOI	61.91	65.74
MgO	4.494	4.670
Al_2O_3	2.624	2.700
SiO_2	14.595	9.871
SO_3	0.628	1.327
K_2O	0.096	0.080
CaO	0.291	0.517
TiO_2	0.100	0.084
MnO	14.640	14.422
Fe_2O_3	0.615	0.579
SrO	0.004	0.004
ZrO_2	0.003	0.004

Table 7. Dried gel phase composition by XRD analysis

Mineral	**Amorphous content**	**Kieserite**	**Szmikite**
Chemical Structure		$MgSO_4.H_2O$	$MnSO_4.H_2O$
	[%]	[%]	[%]
Sample 1	67.9	8.9	23.1
Sample 2	69.9	8.6	21.5

5.8. Ferromanganese slag leach residue: mineralogical analysis and chemical analysis

The residue obtained from this test work mostly contained amorphous microsilica and calcium sulphate species. Moreover, it has already been demonstrated elsewhere (Kazadi *et al*., 2013) that the use of this residue as a Portland cement additive improves the quality of the cement. This residue can also be used as a gypsum replacement to be mixed with clinker during Portland cement manufacturing. The silica content of the residue is beneficial to Portland cement. It is well known that the addition of silica in cement has a positive effect on the cement quality (Bouwers and Radix, 2005; Sobolev et al, 2006; Sobolev and Ferrara, 2005, 2005). The use of this residue in Portland cement improves both the flexural strength and compressive strength of the cement (Kazadi *et al*., 2013).

These residues were obtained using the standard experimental conditions of this study. Table 8 details the typical mineralogical composition of the residues obtained during this test work,

the analyses of which were obtained using XRD. Figure 9 presents a typical XRD spectrum of these ferromanganese slag leach residues.

Table 8. Residue Mineralogical Composition by XRD analysis

Mineral	Amorphous content	Anhydrite	Bassanite	Gypsum	Graphite
Chemical Structure		$CaSO_4$	$CaSO_4.0.5H_2O$	$CaSO_4.2H_2O$	C
	[%]	[%]	[%]	[%]	[%]
Residue 1	41.21	14.91	20.74	23.14	
Residue 2	34.6	1.99		61.55	1.85

Table 9 presents the typical chemical composition, obtained through XRF analysis, of two residue samples. As can be seen from the composition of this residue, its major constituents are the main constitutional compounds (CaO and SiO_2) of Portland cement. The CaO/SiO_2 ratio of this residue is low (0.56), indicating that this residue is a latent hydraulic binder (Mantel, 2001).

Table 9. Residue Chemical Composition by XRF analysis

	Weight Percentage	
Oxide	Sample 1	Sample 2
SiO_2	43.95	39.78
SO_3	27.44	26.99
CaO	24.73	26.27
MnO	1.5	2.73
BaO	1.26	0.817
Al_2O_3	0.262	0.724
MgO	0.158	1.66
Fe_2O_3	0.0984	0.282
K_2O	0.0812	0.0584
Na_2O	0.0692	0.0621

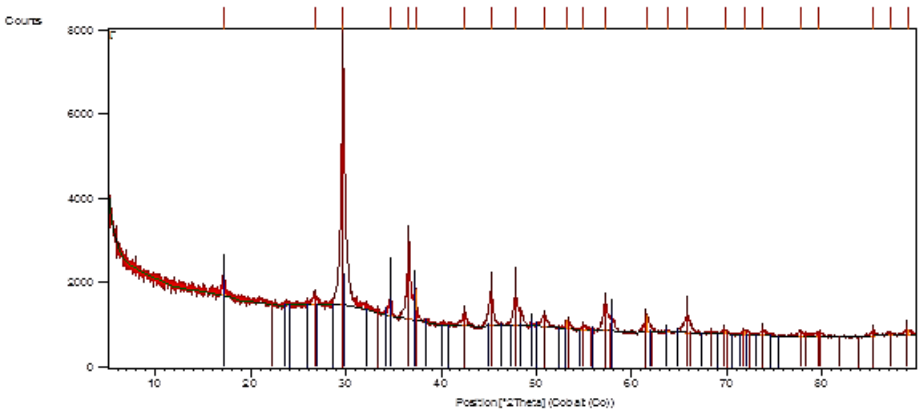

Figure 9. XRD spectrum of ferromanganese slag leach residue (Silicon (20%) was added as internal standard for the determination of amorphous content)

6. Ferromnaganese slag and ferromanganese slag leach residue analysis by scanning electron microscope (SEM).

The structural damage produced by sulphuric acid digestion followed by water leaching of the ferromanganese slag was also studied by SEM. As Suquet (1989) found, acid leaching transformed silicate crystalline phases into very porous, amorphous phases. The crystals are cracked, rendered completely porous and transformed into shapeless material.

Figures 10 and 11 give the micrographs (secondary electron images) of ferromanganese slag and ferromanganese slag leach residue after sulphuric acid digestion and water leaching. In Figure 10 the orthorombic crystal of glaucochroite (centre down) as well as the tetragonal crystal of gehlenite can be seen (top left). In Figure 11, it can be seen how the different crystals have been destroyed by sulphuric acid digestion and water leaching.

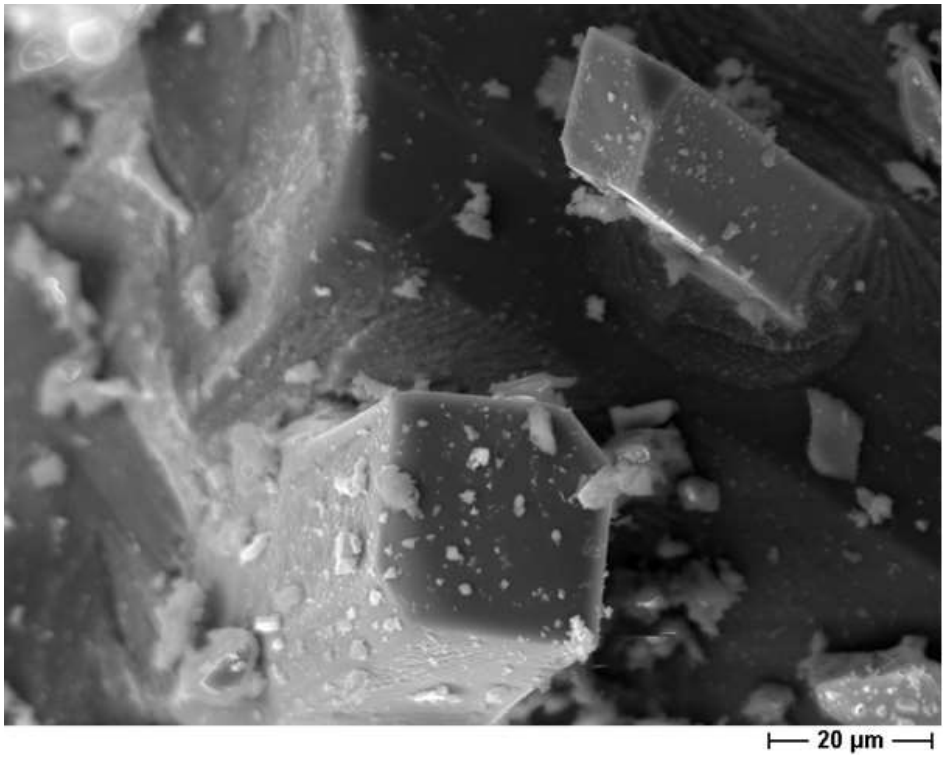

Figure 10. Micrograph (secondary electron image) of ferromanganese slag showing anhydrous glauchochroite and gehlenite

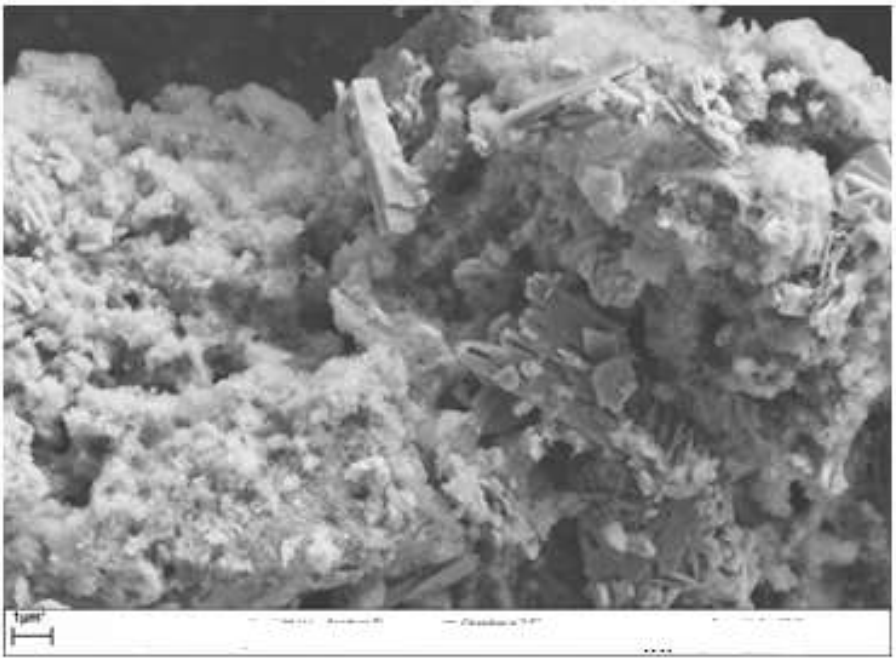

Figure 11. Micrograph (secondary electron image) of ferromanganese slag leach residue showing lathy gypsum crystals and fine grained SiO_2

7. Conclusion

This article shows that it is possible, using hydrometallurgical methods, to limit silica solubilisation and subsequent polymerisation during ferromanganese slag leaching, and to also produce an insoluble residue rich in silica and calcium sulphate species. It further demonstrates the way in which the silica content of the pregnant leach solution (PLS) can be minimised using the quick leach or water-starved theory by rejecting most of silica to the residue. Additionally, it confirms that, by using the reverse of the quick leach theory, silica gel can be produced from ferromanganese slags. The economic viability of the process still needs to be ascertained, in addition to the compilation of a conceptual process flow sheet, which will be addressed in future publications.

Acknowledgments

We would like to acknowledge the initial financial assistance of the BMBF (Federal Ministry of Education and Research, Germany) and the NRF (National Research Foundation, South Africa). We also wish to thank the South African ferromanganese producer for the provision of ferromanganese slag samples. We also thank Henry Honiball and Stuart Silcock from Crosible Filtration for their donation of filter cloths. Our heartfelt thanks also go to Professor

Pöllmann for financial assistance during our visit to the Institute for Geosciences at Martin Luther University, and to Professor De Villiers of the University of Pretoria for facilitating the visit and initiating this project. Finally our heartfelt thanks to Wiebke Grote and Jeanette Dykstra of the University of Pretoria for XRD and XRF analysis and Sabine Walther of Martin Luther University for SEM analysis.

References

1. Baumgartner, S.J., Groot, D.R. 2014. The recovery of manganese products from ferromanganese slag using a hydrometallurgical route. Journal of the South African Institute of Mining and Metallurgy. Vol.114. No.4.pp.331 - 340.
2. Brouwers, H.J., Radix, H.J., 2005. Self-compacting concrete: theoretical and experimental study. Cement and Concrete Research, 35 (2005), pp. 2116–2136. DOI: 10.1016/j.cemconres.2005.06.002
3. Das, S.C., Sahoo, P.K., Rao, P.K., Jena, P.K., 1978. Recovery of manganese value from ferromanganese slag through acid leaching. Trans Indian Inst. of Metals, 31(4) pp. 265 – 267
4. Dufresne, R.E., 1976. Quick leach of siliceous zinc ores. J.Met. 28 (2) (1976) pp.8 -12.
5. Habashi, F., 1993. A textbook of hydrometallurgy. Quebec: Metallurgie Extractive Quebec.
6. Habashi, F. 1997. Handbook of extractive metallurgy. Volume 4 Ferroalloys metals, Alkali metals, Alkaline earth metals. Willey-VCH. Weineheim.
7. Harris, M, Meyer, DM, Auerswald, K., 1977. The production of electrolytic manganese in South Africa. Journal of the South African Institute of Mining and Metallurgy. Vol.077. No.07.pp.137
8. Iler, K.1955. The colloid chemistry of silica and silicate. Ithaca, New York.
9. Kazadi, DM, Groot, DR, Pöllmann H, de Villiers, JPR, Redtmann, T., 2013. Utilization of Ferromanganese Slags for Manganese Extraction and as a Cement Additive. Advances in Cement and Concrete Technology in Africa. Emperor's Palace, Johannesburg, 28 - 30 January 2013. pp. 984 - 985.
10. Lindblad, KO. Dufresne, R.E. 1975. Recovery of metal values from copper slag. US Patent 3868440.
11. Loubser M., Verryn, S. 2008. Combining XRF and XRD analyses and sample preparation to solve mineralogical problems. South African Journal of Geology, Vol.111. No. pp.229-238. DOI: 10.2ll3/gssajg.111. 2-3.229

12. Mantel, DG. 1991. The manufacture, Properties and applications of Portland cement, cement additives and blended cements. Pretoria Portland Cement. The Penrose Press.
13. Murata, K.J. 1943. Internal structure of silicate minerals that gelatinize with acid. The American mineralogist. Vol.28. Nos. 11 and 12. Pp.545-563.
14. Parris, D., 2009. Coagulant training notes Silica in acid leaching. Parris Consulting, Huntsman performance products. Victoria, Australia.
15. Queneau, P.B., Berthold, C.E., 1986. Silica in Hydrometallurgy: An Overview. Canadian Metallurgical Quarterly, Vol. 25. No. 3. pp. 201 - 209. DOI: 10.1179/000844386795430270
16. Sancho, J., Fernández, B., Ayala, J., García, P., Recio, J.C., Rodríguez, C., Bernardo, J.L., 2009. Method of obtaining electrolytic manganese from ferroalloy production waste. 1st Spanish National Conference on Advances in Materials Recycling and Eco – Energy, Madrid, 12-13 November 2009.
17. Seggiani, M., Vitolo, S. 2003. Recovery of silica gel from blast furnace slag. Resources conservation and Recycling 40 (2003) 71 - 80. DOI:10.1016/S0921 - 3449(03)00034-X.
18. Sobolev, K., Ferrara, M., 2005. How nanotechnology can change the concrete world - Part 1. American Ceramic Bulletin, Vol. 84, N°10, (2005), pp. 15-17.
19. Sobolev, K., Ferrara, M., 2005. How nanotechnology can change the concrete world - Part 2. American Ceramic Bulletin, Vol. 84, N°11, (2005), pp. 16-20.
20. Sobolev, K., Flores, I., Hermosillo, R. 2006. Nanomaterials and Nanotechnology for high performance cement composites. Proceedings of ACI Session on Nano-technology of concrete: Recent Developments and Future Perspectives, November 7, Denver, USA, (2006), pp. 91-118.
21. Steenkamp, J.D., Basson, J. 2013. The manganese ferroalloys industry in Southern Africa. Journal of the South African Institute of Mining and Metallurgy. Vol.113. No. pp.667 - 676.
22. Suquet, H. 1989. Effect of dry grinding and leaching on the crystal structure of chrysotile. clays and clay minerals. vol.37. No.5, pp. 439 -445.
23. Takeno, N. 2005. Atlas of Eh-pH diagrams: Intercomparison of thermodynamic databases Geological Survey of Japan Open File Report No.419. National Institute of Advanced Industrial Science and Technology, Research Center for Deep Geological Environments.